Design and preparation of bioactive glasses with hierarchical pore networks†

Hui-suk Yun,* Seung-eon Kim and Yong-teak Hyeon

Received (in Cambridge, UK) 9th February 2007, Accepted 6th March 2007
First published as an Advance Article on the web 16th March 2007
DOI: 10.1039/b702103h

Hierarchically giant-, macro-, and meso-porous 3D bioactive glass scaffolds with good bone-forming bioactivity *in vitro* were synthesized by using a combination of sol–gel, double polymers templating, and rapid prototyping techniques.

Mesoporous materials have attracted much attention as promising host materials for guest organic molecules.[1,2] Recently, the use of these materials in biomaterials science applications, such as drug delivery systems (DDS)[1] and bone tissue regeneration,[2–6] has been proposed. The DDS applications of mesoporous materials have experienced a remarkable breakthrough during the last few years. Scaffolds used for the regeneration of hard tissue constitute another desirable area of applications of mesoporous materials. Their large surface area and pore volume enhance their bioactive behaviour and allow them to be loaded with osteogenic agents promoting new bone formation. The research relating to tissue regeneration has been accelerated following the development of mesoporous bioactive glasses (MBG) by Zhao *et al.* in 2004.[4a] BGs have been widely studied, because they have the ability to chemically bond with living bone tissue and have been used in a variety of medical applications.[7] Increasing the specific surface area and pore volume of BGs may greatly accelerate the kinetic deposition process of hydroxy apatite and, therefore, enhance the bone-forming bioactivity of BGs.[4,5] Zhao *et al.* successfully synthesized highly hexagonally ordered MBGs by templating with a triblock copolymer, $EO_{20}PO_{70}EO_{20}$ (P123) and demonstrated the superior bone-forming bioactivities of MBGs *in vitro* compared to normal BGs.[4] Although MBGs have excellent bone-forming bioactivities, they are impossible to use as scaffolds in tissue regeneration at this stage, because their meso-sized pores are too small to promote cell seeding, migration, and tissue in-growth. Scaffolds with a porous architecture design play a significant role in tissue and should be seriously considered. Suitable tissue scaffolds should have features such as a high porosity with a pore size in the range of 10 to 1000 micrometers and 3D interconnected pore structures to assure a rich blood supply, nutrient delivery and gas exchange, in order to promote the in-growth of bone cells.[8] Herein, we report a novel and reproducible method of preparing hierarchically 3D porous BG scaffolds using a combination of the sol–gel, double polymers templating, and rapid prototyping (RP) techniques, which can generate a physical model directly from computer-aided design data,[9] as shown in Fig. 1. The scaffold is composed of three kinds of scaled pores: meso-sized pores made using a triblock copolymer template ($EO_{100}PO_{65}EO_{100}$ (F127)), macro-sized pores (10 μm $< d_{pore} <$ 100 μm) made using a methyl cellulose (MC) template, and giant-sized pores ($>$ 100 μm) produced by the RP technique (experimental details are given in section S1 in the ESI). Both the giant-sized and the macro-sized pores are designed as biomimicry. The meso-sized pores are additionally added to the scaffold for driving new functionality. The pore size and structures in each size range are designable, controllable and well interconnected. This is the first attempt at the design and preparation of 3D scaffolds which can be used for the regeneration of bone tissue using mesoporous materials. Using this synthetic method, we expect to produce novel functional materials by combining the advantages of the two types of polymer templating methods and the RP technique in various application fields.

Highly ordered MBGs were synthesized using triblock copolymers (F127) as structure-directing. The powder X-ray diffraction (XRD) pattern of the calcined MBG shows three diffraction peaks in the small-angle regime (2θ = 0.95, 1.3, 1.61°), which can be indexed to the (110), (200), and (211) diffractions of a 3D body centred cubic (*Im*3*m*) lattice (Fig. 2a) (d_{100} = 13.1 nm). The transmission electron microscope (TEM) images along the [001] directions also reveal a highly ordered cubic arrangement (Fig. 3a).

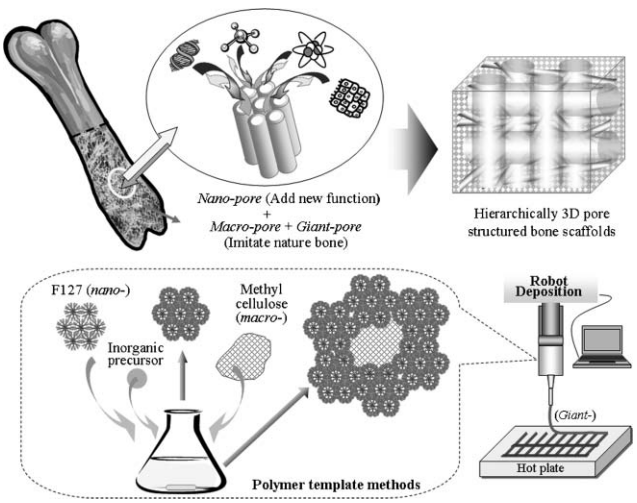

Fig. 1 Schematic illustration of functional scaffolds used for tissue regeneration with hierarchically 3D pore structure (a) and schematic drawing of their synthetic concept (b).

Department of Future Technology, Korea Institute of Machinery & Materials (KIMM), 66 Sangnam-dong, Changwon-si, Gyeongnam, Korea. E-mail: yuni@kmail.kimm.re.kr; Fax: +82-55-280-3399; Tel: +82-55-280-3351

† Electronic supplementary information (ESI) available: Experimental details, schematic illustration of robotic deposition apparatus, optical, SEM, and TEM images of hierarchical pore structures, XRD and quantitative mapping images of scaffold, and SEM images of scaffold after immersion in SBF. See DOI: 10.1039/b702103h

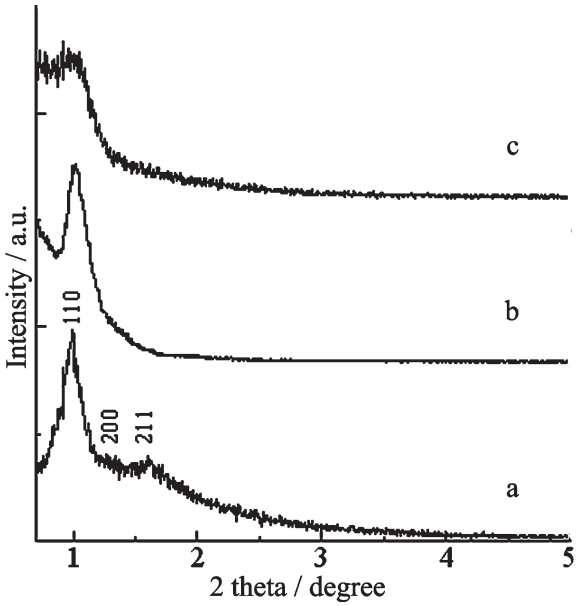

Fig. 2 XRD patterns of MBG (a), meso- and macro-porous BG (b) and meso-, macro-, and giant-porous (c) BG scaffolds.

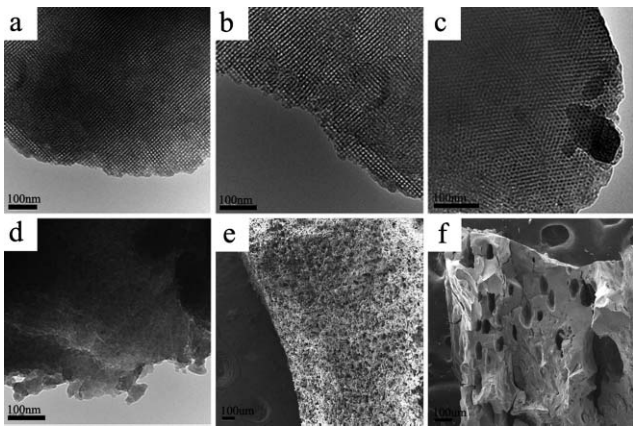

Fig. 3 TEM images of MBG (a), meso- and macro-porous BG (b), and meso-, macro-, and giant-porous BG scaffolds synthesized in the presence of polymer templates (c) and non-porous BG without polymer templates (d). (e) and (f) are the SEM images of (b) and (d), respectively.

The BET surface area, pore volume, and average pore diameter calculated from the nitrogen sorption isotherms were found to be 520 $m^2 \cdot g^{-1}$, 0.51 $cc \cdot g^{-1}$, and 5.4 nm, respectively (more detailed results will be reported elsewhere).

Hydrophilic MC was used as the template for producing additional macro-sized pores in the MBG. The highly ordered cubic-mesostructure was well maintained after mixing the MBG with MC as shown in both Fig. 2b and 3b. It is worth noting that the existence of the triblock copolymer is very effective in producing a uniform distribution of MC in the BG sol solution. According to the results, the macro-sized pores (10–30 μm) were homogeneously produced in the MBG (Fig. 3e), while only heterogeneously distributed giant-sized pores were observed without the triblock copolymer (Fig. 3d and 3f), as shown in the scanning electron microscopy (SEM) results. The development of a method which makes an excludable and geometry-sustainable gel paste plays a key role in the fabrication of scaffolds. The MC plays an important role as a binder and provides the BG sol solution with the rheological characteristics necessary for obtaining structural stability during processing. The BG gel paste so obtained is housed in a syringe for robotic deposition. A low-temperature heating system (60–100 °C) was applied to the substrate used in the RP technique for the purpose of inducing a stable gel structure which comes from both the quick solvent evaporation and the solidification of MC (Fig. S2).

Giant-sized (100–1000 μm) and 3D interconnected pore structures are the main requirement for the scaffolds used in tissue regeneration. Several kinds of 3D-scaffold structure were designed by a computer as shown in Fig. 4 (a–c, upper line). The cuboid scaffold in Fig. 4a is designed as a lattice of rods stacked with simple tetragonal symmetry. Fig. 4b shows a lattice of rods stacked offset with the same tetragonal pattern of Fig. 4a. Fig. 4c shows a lattice of rods stacked as in Fig. 4b but with layers having different orientations. Changing the buildup mode while retaining the same lattice pattern allows both the pore sizes and structure to be changed. The pore size of structures b and c is a quarter of that of structure a. A cylindrical geometry can be fabricated as well (not shown here). Each designed scaffold was well produced with the BG gel paste (Fig. 4 middle line). 20 layers of the lattice were stacked (total thickness = 7 mm) with base dimensions of 20 × 20 mm. The interstitial distance between the struts was 2 mm. These values do not represent the process limits. The size, thickness and structure of the scaffold can be easily managed under computer control. The pore sizes can be adjusted by changing the design of the pore structure (above 100 μm). The strut size of the extruded gel paste is also important to obtain favourable pore sizes and structures, and largely depends on both the nozzle size and the scanning speed. The nominal feature size of the extruded nozzle was in the range of 17 to 28 gauge (G) (24 G (≈500 μm) was generally used here) and the scanning speed was in the range of 5 to 10 $mm \cdot s^{-1}$. These structures were well maintained even after removing the polymer templates, with no structural deformation

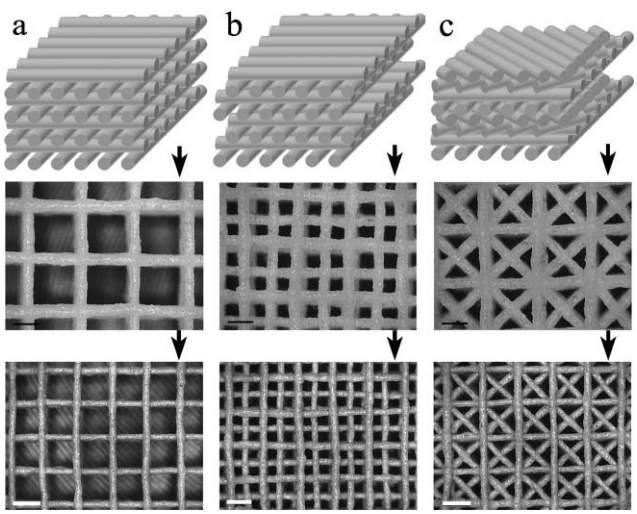

Fig. 4 3D periodic scaffolds with simple tetragonal geometry (a), with tetragonal geometry with offset layers (b) and with decussated structure (c). Schematics of designed images (upper line) and optical images of as-synthesized gel scaffold (middle line) and calcined hierarchically porous scaffold (bottom line). (bar = 1000 μm).

caused by the calcination at 600 °C (bottom line), although it caused an approximately 35% decrease of the scaffold size, due to the condensation of the BG frame. After calcination, the pore sizes decreased from 1500 μm to 970 μm for Fig. 4a and from 600 μm to 390 μm for Fig. 4b. The larger spacing between adjacent lines within a layer results in an increase in the pore size and volume fraction. It is worth noting that each calcined strut, which forms a giant pore, contains both a meso-structured pore and a macro pore (Fig. 2c, Fig. 3c and Fig. S3). The 3D pores of each size were open and continuously connected, *i.e.*, all of the pores likely contribute to the effective surface area. Though only one XRD diffraction peak was obtained, owing to the decrease in the long pore arrangement, the TEM image along the [$\bar{1}$11] direction showed that the 3D scaffold still had a 3D *Im*3*m* mesostructure (Fig. 3c). As a result, a novel hierarchical meso-, macro-, and giant-porous BG scaffold was successfully obtained by the combination of the two preparative methods for porous materials (Fig. 1b and Fig. S3). In addition, the results of both WAXRD and quantitative mapping from TEM revealed that the Ca and P species were distributed homogeneously in the silica network on the nanoscale (Fig. S4).[4b]

The bone forming activity of the hierarchical porous BG scaffold *in vitro* was tested in simulated body fluid (SBF) to monitor the formation of hydroxyl apatite (HA) on the surface of the scaffold. The SEM image of the scaffold before soaking shows a smooth and homogenous surface (Fig. S5a). The SEM image reveals that the surface of the scaffold undergoes important changes when it reacts with SBF. After 24 h, the scaffold is fully covered by a new apatite-like phase composed of rod-like particles with a length of around 100 nm, which is similar to the morphology of HA in human bones (Fig. S5b). The biomimetic HA formation behaviour of the hierarchical porous scaffold means that the scaffolds synthesized by the current strategy possess outstanding bone-forming activity *in vitro*.

In summary, hierarchical 3D porous BG scaffolds with highly ordered mesoporous structures were prepared using a combination of the synthetic methods used for the fabrication of two types of polymer templates and RP. The good bone-forming bioactivity of these scaffolds *in vitro* was also confirmed. Their mesoporosity should enhance the tissue oxygenation and enable the possibility of introducing different drugs for controlled release. We hope that this simple, reproducible synthetic method can be adapted for the preparation of various hierarchical porous materials, having the potential to be used in applications involving functional scaffolds used in tissue regeneration, sensors, catalysis, and optics.[10] More detailed structural investigation of these hierarchical porous scaffolds, and studies of their mechanical, and both *in vitro* and *in vivo* properties are currently in progress.

Notes and references

1 M. Hartmann, *Chem. Mater.*, 2005, **17**, 4577.
2 W. Xia and J. Chang, *J. Controlled Release*, 2006, **110**, 522.
3 (*a*) M. Vallet-Regí, *Chem.–Eur. J.*, 2006, **12**, 5934; (*b*) M. Vallet-Regí, L. Ruiz-González, I. Izquierdo-Barba and J. M. González-Calbet, *J. Mater. Chem.*, 2006, **16**, 26.
4 (*a*) X. Yan, C. Yu, X. Zhou, J. Tang and D. Zhao, *Angew. Chem., Int. Ed.*, 2004, **43**, 5980; (*b*) X. X. Yan, H. X. Deng, X. H. Huang, G. Q. Lu, S. Z. Quio, D. Y. Zhao and C. Z. Yu, *J. Non-Cryst. Solids*, 2005, **351**, 3209; (*c*) X. Yan, X. Huang, C. Yu, H. Deng, Y. Wang, Z. Zhang, S. Qiao, G. Lu and D. Zhao, *Biomaterials*, 2006, 3396.
5 (*a*) I. Izquierdo-Barba, L. Ruiz-González, J. C. Doadrio, J. M. González-Calbet and M. Vallet-Regí, *Solid State Sci.*, 2005, **7**, 983; (*b*) A. López-Noriega, D. Arcos, I. Izquierdo-Barba, Y. Sakamoto, O. Terasaki and M. Vallet-Regi, *Chem. Mater.*, 2006, **18**, 3137.
6 (*a*) Q. Shi, J. Wang, J. Zhang, J. Fan and G. Stucky, *Adv. Mater.*, 2006, **18**, 1038; (*b*) T. A. Ostomel, Q. Shi, C. K. Tsung, H. Liang and G. D. Stucky, *Small*, 2006, **2**, 1261.
7 (*a*) L. L. Hench, R. J. Splinter, W. C. Allen and T. K. Greenlee, *J. Biomed. Mater. Res.*, 1971, **2**, 117; (*b*) L. L. Hench, *J. Am. Ceram. Soc.*, 1998, **81**, 1705; (*c*) L. L. Hench and J. M. Dolak, *Science*, 2002, **295**, 1014.
8 S. J. Hollister, *Nat. Mater.*, 2005, **4**, 518.
9 B. Xie, R. L. Rarkhill, W. L. Warren and J. E. Smay, *Adv. Funct. Mater.*, 2006, **16**, 1685.
10 P. Gómez-Romero and C. Sanchez, *Functional Hybrid Materials*, Wiley-VCH, Weinheim, 2003.